STRUCTURAL SCIENCE
CRYSTAL ENGINEERING
MATERIALS

Volume 76 (2020)

Supporting information for article:

Cation distribution in Cu2ZnSnSe4, Cu2FeSnS4 and Cu2ZnSiSe4 by multiple-edge anomalous diffraction

Daniel M. Többens, Galina Gurieva, Sara Niedenzu, Götz Schuck, Ivo Zizak and Susan Schorr

1) Experimental MEAD data

MEAD experimental data and corrections are stored in tables in ASCII format with 10 columns each. The data columns contain:

1 Radiation energy E in keV

2 Radiation wavelength in Angstrom, as calculated from E

3 Position of Bragg peak in Q-space [in $Å^{-1}$]

4 Intensity Int_{raw} of Bragg peak derived as the area of a Gaussian fitted with common FWHM to the complete energy range

5 Background fitted at the peak position

6 Linear absorption coefficient μ [in cm^{-1}] as calculated from the tabulated values according to the table below

7 Linear absorption coefficient μ_{shift} as in (6), but calculated from slightly shifted energy values in order to consider the shift of the absorption edge evidenced by the onset of increased background from fluorescence

8 Transmission factor T_{air} in air, calculated for a distance of 90 cm between monitor counter and detector. The function T_{air} = exp(-(4832.25323*E^-2.97468)*0.001225*90) used was fitted to published data (Hubbell, 2004)

9 Intensity correction $C_Q = 4asin(Q\,\lambda/4\,\pi)/Q$ for the transformation into Q space. The intensities are correct in 2θ, but fitting in Q was done for practical reasons.

10 Final corrected intensity $Int_{raw}\ \mu_{shift}\ C_Q / T_{air}$, normalized to an average value of 100 for the whole observation range

Data are provided for

CFTS Cu_2FeSnS_4, Bragg peaks 002, 011, 110

CZTSe $Cu_2ZnSnSe_4$, Bragg peaks 002, 011, 110

CZSiSe $Cu_2ZnSiSe_4$, Bragg peaks 110, 101, 011, 111, 200

Hubbell, J. H. S., S. M. (2004). *X-Ray Mass Attenuation Coefficients - NIST Standard Reference Database 126*.

2) Illustration of the Rock-in-the-Dust effect on MEAD data

If a powder sample consists of too large grains, this results in spottiness of the Debye rings. This effect is especially strong at instruments with very low beam divergence, as is the case for most synchrotron diffractometers. Rotating the sample decreases this problem. This was done in all experiments presented in this paper, with the exception of CZTSe, whose MEAD data had been collected first. In most cases, it still would not have been a problem, as the sample is tilted in accordance with the changing radiation energy so that always the same grains remain in reflection conditions. A strong grain might cause a shift in overall intensity, without changing the characteristic energy dependency. However, in this case a strong spot appeared very close to the edge of the observation range. As diffraction angles decrease with decreasing wavelength, the shrinking diameter of the Debye ring brought this spot over the edge inside the observation range. Fortunately, this can normally be noticed.

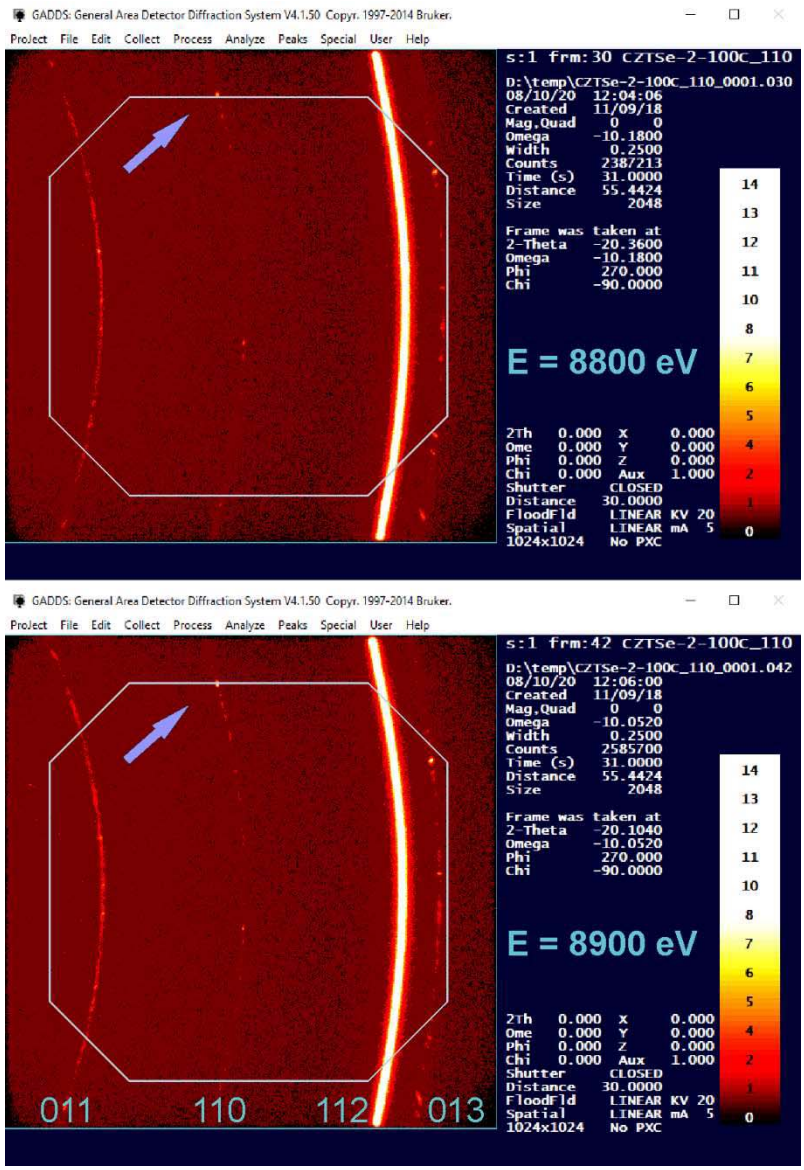

Figure S1. A particularly strong spot in the 110 Debye ring of CZTSe is located right at the electronically defined limit of the observation range, which excludes data of lower quality at the edge of the detector.

Table S1 Structural parameters of $Cu_2ZnSiSe_4$ with experimental composition $Cu_{1.935}Zn_{0.975}Si_{1.029}Se_4$ when refined as stoichiometric.

Atom	*x*	*y*	*z*	U_{iso} / Å^2	*s.o.f.*
Cu1	0.7491(14)	0.8281(8)	0.6390(10)	0.0130(4)	0.877(30)
Zn1	0.7491(14)	0.8281(8)	0.6390(10)	0.0130(4)	0.123(30)
Cu2	0.7430(15)	0.1787(8)	0.1259(12)	0.0130(4)	0.123(30)
Zn2	0.7430(15)	0.1787(8)	0.1259(12)	0.0130(4)	0.877(30)
Cu3	0.0025(16)	0.6508(3)	0.1281(11)	0.0159(7)	1.00
Si4	0.00	0.3261(6)	0.625	0.0078(9)	1.00
Se5	-0.0054(13)	0.64382(19)	0.5015(8)	0.0106(4)	1.00
Se6	-0.0017(12)	0.3204(2)	-0.0201(8)	0.0126(4)	1.00
Se7	0.7406(14)	0.8297(6)	0.0098(8)	0.0056(7)	1.00
Se8	0.7598(13)	0.1699(6)	0.5088(10)	0.0151(9)	1.00
Lattice parameters					
a = 7.824323(16) Å		b = 6.730624(12) Å		c = 6.450762(15) Å	
β = 90.0660(2)°		V = 339.7135(12) Å^3			